International Journal of Engineering Trends and Technology
ISSN: 2231 – 5381 /doi:10.14445/22315381/IJETT-V69I8P206
Volume 69 Issue 8, 41-48, August, 2021

Measurement of Electrical Resistivity of Powder; Comparison of Three Methods

Adoum Traoré Ndama[#1], Elysée Obame Ndong[#2], Yves Constant Mombo Boussougou[#3], Gaston N'Tchayi Mbourou[#4]

[#] *Electrical Engineering Laboratory (M2elab), Ecole Polytechnique Masuku de l'Université des Sciences et Techniques de Masuku, Mbaya, route nationale, BP 941, Franceville, Gabon*

[1]adoum.traore-ndama@univ-masuku.org, [2]elysee.obame@univ-masuku.org

Abstract *— The use of powder dielectric material in industrial applications is responsible for electrostatic charge accumulation, which can cause damages such as fires or explosions. In this paper, we present three different methods for the characterization of the resistivity of powders. The first method is based on Ohm's Law. The sample of powder to be tested is placed in a measuring cell between two electrodes subjected to high DC voltage. The second method is the AC resistivity measurement, which makes use of an LCR-meter, and the third method is the measurement of surface resistivity by the decay of charge over time. The results obtained show a match between these techniques as a function of the batches of powder and a considerable dispersion for some others. Indeed, the results obtained have shown that the AC method is better for size measurement of irregular glass beads and the DC method is adequate for size measurement of spherical glass beads. As for the results found by the charge decay method under the same conditions of temperature and relative humidity, they differ from others in 10^4 times more important. For charge decay measurement, it has been shown that the shape of the glass beads does not significantly influence the resistivity results.*

Keywords *— electrical resistivity, powder dielectric material.*

I. INTRODUCTION

The Characterization of the electrical properties of a powder proves to be of greater importance given its manipulation and its growing involvement in the processes. Although the effects of electrostatic charge accumulation within particle surfaces have several industrial advantages, such as the electrostatic separation [1, 2] of materials, they also have several disadvantages. Indeed, during the last decades, many industrial installations or processes using insulating materials have been victims of fire or explosion [3, 4], affecting the process performance and endangering the equipment or operators, especially when processing flammable materials [5–8]. It is partly in the growing use of the powder material that the electrostatic risks have become of concern. Thus, it is preferable to electrically study a powder before it is used in industry. It is generally thought that decreasing resistivity also decreases charging [9]. This information could be interesting to link the behavior tribochatrging of particles and their electrical properties.

However, there are several methods for measuring the electrical properties of powders in the literature. In this work, we are interested in the measurement of electrical resistivity of powders; three different measurement techniques. The first is the DC electrical resistivity measurement using a device comprising an electrical diagram particularly composed of a programmable high voltage power supply via a computer and a measuring cell (CHIWORTH cell or 16452 A cell). The second method is the AC resistivity measurement, which particularly includes a device delivering a sinusoidal voltage (LCR-meter) and a cell in which the powder sample is placed (cell 16452 A). And finally, the measurement of surface resistivity by the decay of charge in time (Chubb cell, JCI 155 v) [10]. Note that devices existing in industries and are based on the same principle.

II. MATERIALS AND METHODS

A. *Materials*

Different types of powders were used to carry out this study. The choice of these powders is due to the fact that they are widely used in industry, easy to use, and to be distributed according to the different particle size distributions in irregular and spherical shapes. Moreover, they are widespread in the trade of which is easy to acquire. The first measurements were made on four types of spherical glass beads powders with sizes ranging from 75 and 150µm, 80 and 100µm, 150 and 250µm, and 250 and 500µm. The second batch of four types of powders is non-spherical-shaped glass beads of sizes corresponding to the first batch. (Fig. 1 on the preparation of these batches of powder)

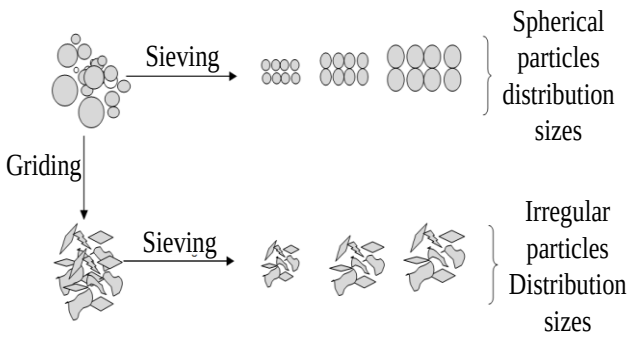

Fig. 1 Preparation of powders in different sizes and shapes

The accuracy of the characteristic dimensions of the batches of powders as well as the particle size distribution was determined by laser diffraction using the Malvern Mastersizer (apparatus constructed by Malvern Instruments). In addition, the relative humidity conditioning HR (%) and temperature T (°C) were controlled in the glove box JCI 191 controlled Humidity Chamber John Chubb Instrumentation. The size and morphology of the particles used can be seen in the scanning Electronics Microscopy (SEM) images presented in Fig. 2.

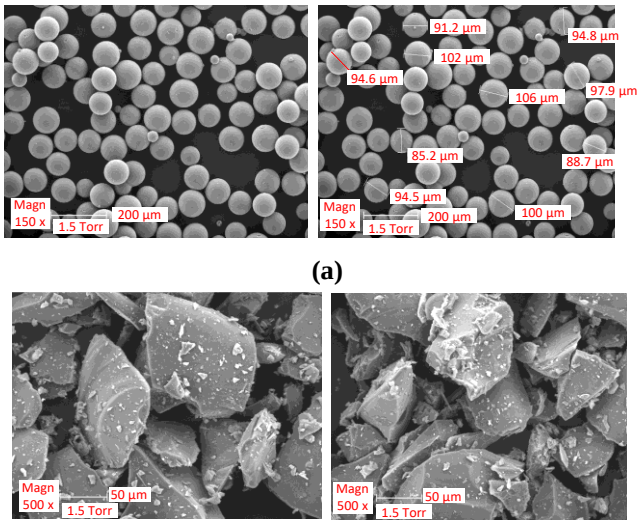

(a)

(b)

Fig. 2. SEM Images of powder particles: (a) spherical glass beads; (b) of non-spherical glass beads

B. Measurement methods

The resistivity of a compact material or a powder is defined as the ability of this latter to oppose the passage of the electric current expressed in Ω.m. It is strongly dependent on the temperature [11] and relative humidity [12–15]. The measurement techniques used in this paper are those for the measurement of volume and surface resistivity.

a) DC measurement method: The measurement of the resistivity of the powders is carried out in a cell, between two electrodes on which the sample is placed (see Fig 3). The geometry of the cell being fixed is characterized by a constant geometric C which is the ratio of the surface of the electrodes and the thickness separating them. The resistance R of the cell containing the powder is determined from the measurement of the current flowing between the electrodes when a known potential difference (0 to 10 kV and a fixed intensity of 1 mA) is applied between these electrodes. Therefore volume resistivity noted ρ_V is given by the relation (1).

$$\rho_V = R \times C \tag{1}$$

For that measurement, the assembly used is composed of the following elements:

- HV electrical feeder (Spellman Modal SMS 60P60 - 60KV, 60W, 1mA, 24VDC, positive polarity) whose computer programming was developed by the electronic service of UTC (University of Technologie of Compiègne). The resistivity cell (Chilworth cell manufactured by the company Chilworth Technology or cell 16452 A developed by Hewlett Packard) is composed of two flat electrodes; the lower electrode is integrated into the cell, and an upper electrode is connected to the high voltage supply. The constant of the Chilworth cell is 0.4 m, and that of the measuring cell 16452 A is 0.57 m.
- Pico ameter Keithley connected at the lower electrode.
- A programming computer for high-voltage power and data acquisition. (Fig. 3).

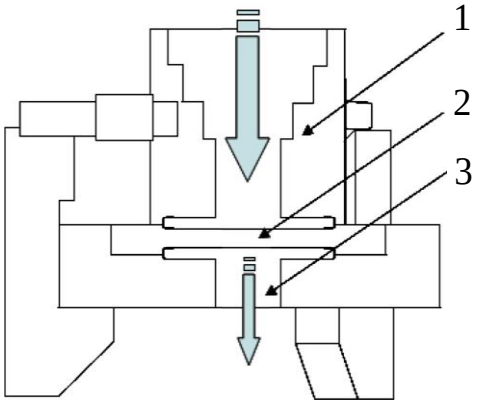

Fig. 3. Chilworth cell: (1) upper electrode, (2) powder loading location, and (3) lower electrode.

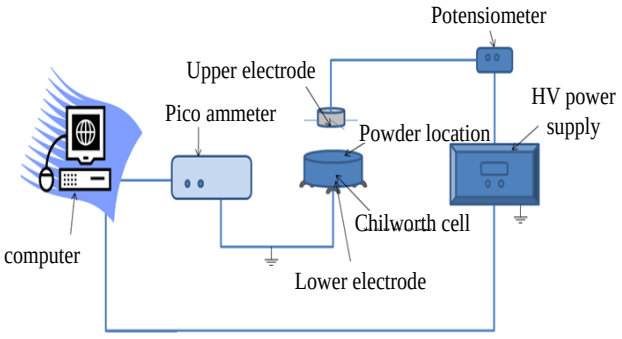

Fig. 4. DC resistivity measurement diagram.

b) A measurement method: The use of alternating voltage permits to characterize the different resistive and capacitive behaviors of the device to be studied. This technique, known as impedance spectroscopy, widely used in the electrochemistry of liquids, has been adapted to the study of solids [16, 17]. The technique consists of working with an alternating current I = I0 exp. i (ωt+φ) resulting from a sinusoidal voltage U of pulsation ω. This sinusoidal current undergoes in the sample a phase shift φ related to the presence of the capacitive elements. The I/U ratio is then defined as the system impedance Z (φ)= Z_0 exp (-iφ). It is, therefore, a complex number composed of a real part Re (Z) and an imaginary part Im (Z). Thus, the displacement of the charge carriers in the grains that are occurring at the joints will be distinguished. The first is considered as a purely resistive phenomenon, and the second is a resistive-capacitive system. So, in general:

- The low frequencies are essentially representative of capacitive phenomena that may occur at the electrodes;
- Intermediate frequencies are essentially representative of the capacitive and resistive phenomena that may occur at grain boundaries;
- The high frequencies are essentially representative of the resistive phenomena that can occur inside the grains (intra-granular phenomenon).

Such behavior can be illustrated by constructing and calculating an electrical circuit consisting of two resistors, R and r, and a capacitance C (Fig. 5). Thus, R and C are connected in parallel, and r is arranged in series with respect to this RC circuit; the impedance of the circuit is calculated by using the relation (2).

$$Z_{CIRC} = r + Z_{II} \tag{2}$$

where

$$Z_{II} = \frac{iR}{i + R\omega C} \tag{3}$$

thus we obtain the relation (4)

$$Z_{CIRC}(\omega) = \left(r + \frac{R}{1 + (\omega\tau)^2}\right) - i\left(\frac{R\omega\tau}{1 + (\omega\tau)^2}\right) \tag{4}$$

with τ=RC, time constant of the RC parallel circuit

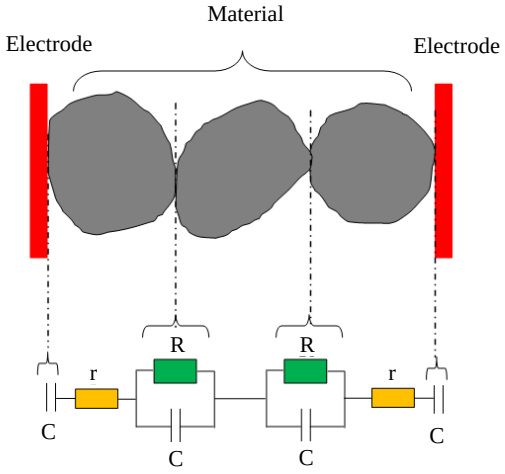

Fig. 5. Electrical circuit modeling of interface phenomena.

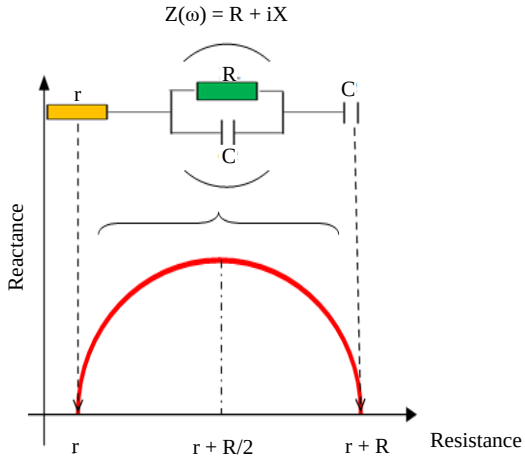

Fig. 6. Diagram of Nyquist.

Two particular areas of the graph are to be considered (Fig. 6):

- The points of intersection of the semicircle intersect the abscissa axis at (r + R) when the frequency is zero and at r when the frequency tends to infinity. R represents

the resistance of the system and r the resistance of a grain. This information allows to determine the contribution of each resistive element of the device;

- Another particular point is the peak of the arc having for abscissa r + R/2 reached for the frequency f_0 (with $f_0 = 1/(2\pi RC)$) that is the relaxation frequency;

Measurements were realized by AC measurement device (Fig. 7) using an LCR Meter capacitor 4284A from Hewlett Packard Company which connected to the resistivity cell 16452A by connection cables. The sample is placed inside the cell without the thickness exceeding 2 mm so as to keep the geometric factor constant (FG = 0.57 m). This device allows a frequency sweep between 20 Hz and 1 MHz, and a maximum voltage amplitude is set at 100 mV.

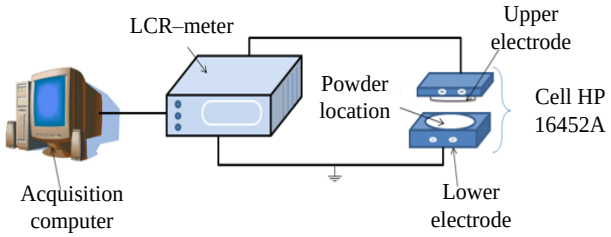

Fig. 7. Experimental setup for AC measurement.

***c) Measurement method by charge decay*:** Electrical resistivity of materials with electrostatic hazards is generally linked in area resistivity measurement. The resistivity values allow us to determine the ease with which materials are able to hold or dissipate charges. Electrical charges flowing are proportional to the voltage of condensation and so on the remaining charge. Therefore, the charges rapidly decay at the start when the charge is high and slowly when the charge and voltage are low. The relationship between charge rate flow, capacitance, and voltage leads to an exponential decay of charge, which is translated mathematically by relation (5).

$$q = q_0 e^{-t/\tau} \tag{5}$$

where q stands for charge in time t, q_0 accounts for an initial charge, and τ is the time constant which represents the time to reach approximatively 37 % of the initial charge.

In general, the decay curve differs from an exponential (as a result of the variation in the resistivity of material as a function of an electric field) and can be very complex for heterogeneous materials. However, whether the logarithm of q as a function of time is plotted, one obtains slope right -1/τ. The time constant will be obtained experimentally from charge decay measurement as a function of time expressed by the mathematical relationship (6).

$$\tau = \varepsilon_r \varepsilon_0 \rho \tag{6}$$

Where ε_r accounts for dielectric constant and ρ material resistivity (see for example in Fig. 8 charge decay obtained with powder sample of PVC).

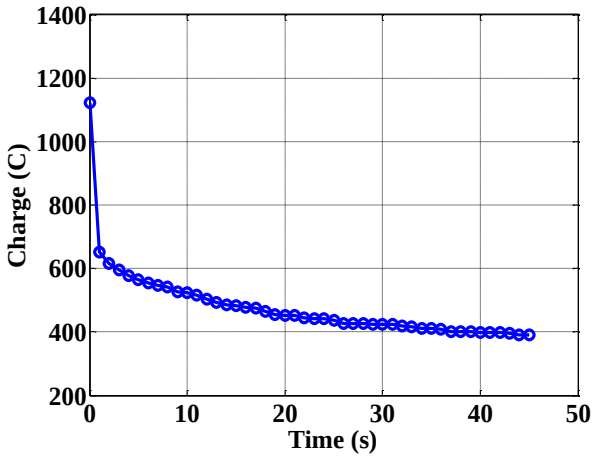

Fig. 8. Charge (C) decay obtained with pvc powder (Operating conditions: Corona Voltage: -10 kV, T° = 17,6 °C, HR = 34,67%).

Charge decay over time is directly related to the resistivity value of the material. Note that several apparatuses exist in the market to permit this measurement. One of these devices was developed by John Chubb Instrumentation society: JCI 155 charge Decay Meter (Fig. 9).

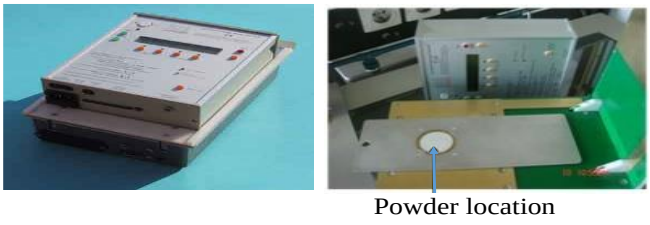

Fig. 9. JCI 155 charge Decay Meter.

The measurement consists of generating a high voltage corona discharge (3 to 10 kV) as a short pulse (10 ms) on a material placed in an aluminum location. After generation of the corona discharge, the movable plate supporting the electrodes is removed very quickly, thus making possible the measurement generated by a field mill (Fig. 10).

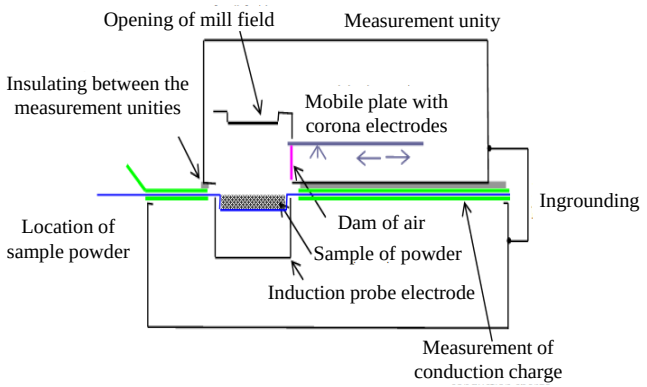

Fig. 10. JC I 155 cell: the principle of measurement.

An acquisition software designed allows recording the evolution of the voltage as the charges are evacuated. The field mill has a response time of less than 10 ms and a charge decay time between 50 ms and several days.

III. RESULTS AND DISCUSSION

Temperature and moisture strongly affect powders' resistivity [18, 19]. For this reason, our measurements were achieved with controlled temperature and moisture. We used a glove box JCI 191 controlled humidity chamber of John Chubb Instrumentation. In addition, all measurements were repeated several times to value the reproducibility of our tests.

A. Measurement according to the particles size distribution

***a) DC measurement*:** For all samples, resistivity values were calculated from the average value of current measured 60 seconds after each applied voltage level. Fig. 11 show the behavior of current as a function of applied voltage for different size of spherical glass beads. One can observe that current increases logically against applied voltage, and this increase is strengthened with the increase of the size of the beads. In Fig. 12, it is observed that electrical resistivity decreases with applied voltage. However, the resistivity seems to decrease with the increase in spherical beads size.

The decrease of resistivity with the increase in spherical beads size could be due to the occupation of air in the space between the neighbor particles. Since air is more resistive than glass, its presence would affect the complete resistivity of the sample because the larger the particle sizes, the more zones of larger air space are formed [20]. Also, the phenomenon of purification (decay in time of the current passing through the sample) seems more important for samples made of fine particles, which is explained by the fact that, for a given volume of material, the overall surface of the particles is inversely proportional to the average radius of these particles [21].

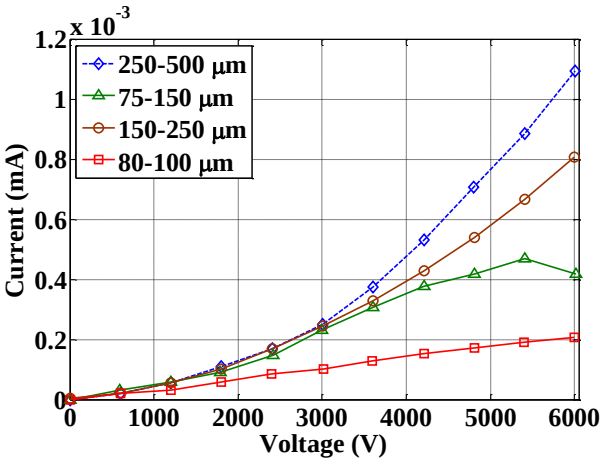

Fig. 11. Current as the function of applied voltage for spherical glass beads.

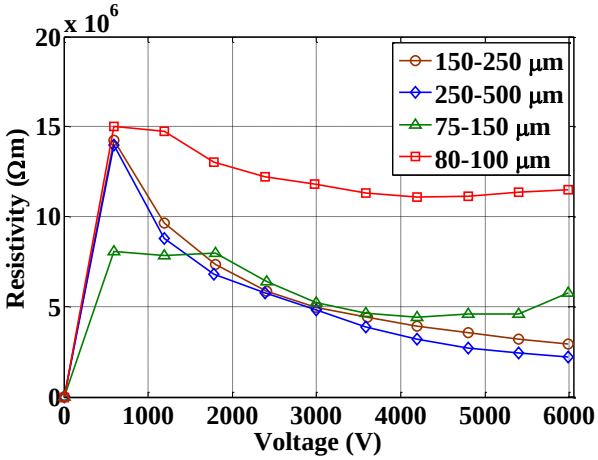

Fig. 12. Resistivity versus applied voltage for spherical glass beads.

***b) AC measurement*:** Each measurement was carried out from sinusoidal voltage whose frequency sweep is between 20 Hz and 1 MHz. The resistivity measurement corresponds to the point of intersection between the curve and the x-axis multiplied by constant geometric FG = 0,57 (16452 cells). As can be seen in Fig.13, the glass beads of (150-250µm) present a higher resistivity value than the other particle size distributions. As we can see between the different particle size distributions (80-100 µm, 75-150 µm, and 150-250 µm), the larger the particles, the higher the measured resistance value.

Nevertheless, it is observed that for particle sizes (250-500µm), the resistivity value is less important than the batch 150-250 µm. This scattered for the glass beads (250-500 µm) can be explained by the fact that it is possible that when the standard cell was used, a significant amount of current was able to flow to the current electrode via the path outside the volume between the electrodes [9]. This method does not significantly identify the influence of the particles size for spherical glass beads.

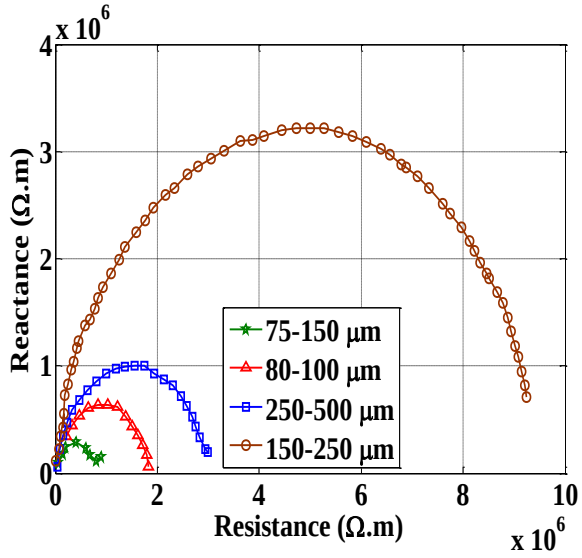

Fig. 13. Complexes impedances diagram spherical glass beads in different size distributions.

B. Measurement as a function of particles shape

a) DC measurement

The measurements were performed several times to reassure ourselves of the repeatability of our measurement tests. TABLES I and II show the influence of the shape of the sample on the resistivity value. It can clearly be seen that the resistivity values of non-spherical-shaped glass beads are larger than those of spherical ones. This could be due to the significant decay of the electric current in the time observed during our measurements. Indeed, the potential difference arising between the two electrodes of the cell containing the powder sample creates a bias current which generates an electric field opposite to that formed by the potential difference. This result gives a link of powder turbocharging behavior in literature where the authors clearly show that the largest charge is reached with the irregularly shaped particles in pneumatic conveying and concluded that this phenomenon is due to a larger surface area of the angular particles [22, 23].

TABLE I. Resistivity of the size distribution of spherical glass beads

spherical glass beads diameter [µm]	**[80 - 100]**	**[75 - 150]**	**[150 - 250]**	**[250 - 500]**
Resistivity (MΩ.m)	12 ± 10	6 ± 2	3 ± 1	2 ± 14

TABLE II. The resistivity of sizes distribution of nonspherical glass beads

Sizes distribution of non-spherical glass beads [µm]	**[80 - 100]**	**[75 - 150]**	**[150 - 250]**	**[250 -500]**
Resistivité (MΩ.m)	20 ± 10	7 ± 2	3.8 ± 1	4 ± 14

b) Charge decay measurement

In TABLE III, we have mentioned results obtained for irregular and spherical glass beads from the charge decay measurement. As be seen, the resistivities values of the two batches of glass beads of the same size are almost the same because it is a surface measurement whose component shape does not affect the resistivity.

TABLE III. The resistivity of spherical and non-spherical glass beads for four-particle size distribution with JC I 155 cell

Particle size distribution [µm]	**[80 - 100]**	**[75 - 150]**	**[150 -250]**	**[250 -500]**
The resistivity of spherical glass beads ($\Omega.m\times10^{11}$)	-	5,21 ± 0,6	3 ± 0,4	7,84 ± 0,1
Resistivity of non-spherical glass beads ($\Omega.m\times10^{11}$)	4,27 ± 0,5	5,41 ± 0,3	3,5 ± 0,45	7,84 ± 0,1

c) AC measurement

The results obtained by complex impedance as shown in Fig.16 that samples of glass beads of non-spherical shapes of different sizes have specificities related to the polarization of the electrodes. It appears for the high frequencies of measurement an additional semi-circle (Fig. 14) for some samples that can be attributed to the conduction mechanism inside the grains [24]. As we can see in Fig. 15, except for the batch 250-500 µm, resistivities obtained with spherical glass beads are more important to the measurement obtained by the AC method. We constate that contrary to the DC method, the trend of increasing resistivity in the function of size distribution particles for the non-spherical glass beads is observed.

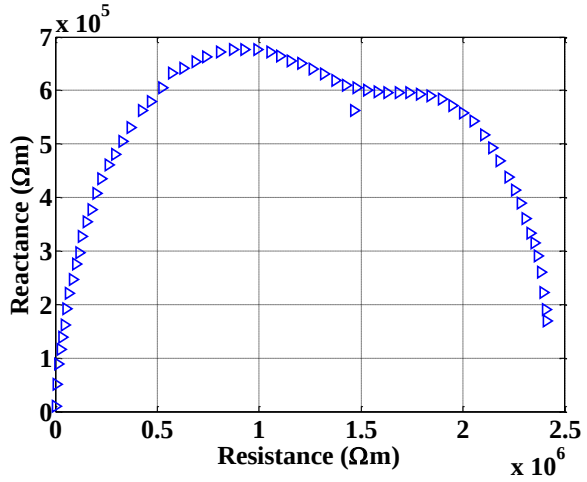

Fig. 14. Complexes impedances diagram of non - spherical glass beads (150 - 250µm).

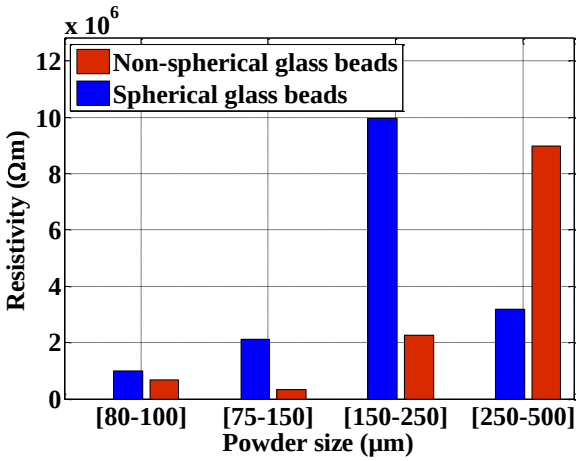

Fig. 15. Resistivity for AC method for non-spherical and spherical beads for different size distributions.

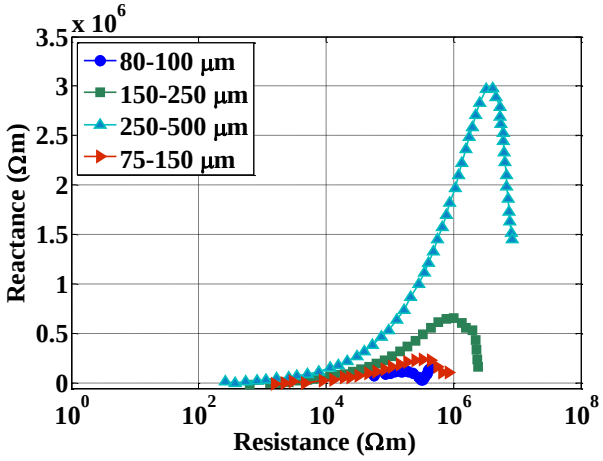

Fig. 16. Complex impedance diagram of the batch of non-spherical glass beads *(logarithmic scale)*

IV. CONCLUSIONS

This study presents the results of electrical resistivity tests of powders using three different measurement methods. It could be to increase the knowledge in the field of turbocharging of powder which doesn't really apprehend and cause several damages in processes. Note that a good protocol for measurement of electrical properties of powder could be permitted to predict their aptitude for taking electrical charge during its handled. We have highlighted the particle size distribution and the shape of the samples according to the measurement methods used.

- According to the size distribution of powder, the DC method could be adequate to do measurements of spherical glass beads and the AC method for non-spherical glass beads. However, the AC method does not permit significantly identify the influence of the particle size of spherical glass beads and the DC method for non-spherical glass beads. As for the measurements obtained by the charge decay method, there is a limit in the procedure for determining the electrical resistivity. Indeed, this method is applicable for samples with resistivity values greater than 1010 Ω.m. This result is a good agreement with the literature, where it is well established that surface resistivity can exceed volume resistivity by several orders of magnitude.
- According to the shape of particles, resistivity values of non-spherical shaped glass beads obtained by the DC method have given the results more important than spherical glass beads. Nevertheless, the AC method has shown that the shape does not affect the resistivity value as it might for other volume measurements. The results obtained by the charge decay method have shown that for all batches of glass beads of the same size and different shapes, the resistivity values remain almost the same because it is a surface measurement whose shape of the component does not affect the resistivity value.

It will be interesting for the next work to improve the protocols of measurement to ensure the reliable measurement of powder in order to link the tribochatrging behavior of powders and their electrical properties.

Acknowledgments

The authors thank Prof. Lucian Dascalescu and Prof. Eloi Blampain for fruitful discussions and valuable suggestions regarding the goals of research in general.

REFERENCES

[1] A. Iuga, S. Vlad, M. Mihailescu, and L. Dascalescu, A laboratory plate/screen–type electrostatic separator for granular mixtures design, engineering and applications, Particulate Science and Technology, 22 (3) (2004) 275–283.

[2] A. Younes, M. Younes, H. Sayah, A. Samuela, and L. Dascalescus, Experimental and numerical modeling of a new tribo-electrostatic separation process for granular plastics mixtures, Particulate Science and Technology, 33(2) (2014) 189–196.

[3] A Ohsawa., Computer simulation for assessment of electrostatic hazards in filling operations with powder, *Powder Technol.* 135–136, 216–222 (2003).
[4] M. Nifuku and H. Katoh, A study on the static electrification of powder during pneumatique transportation and the ignition of the dust cloud, Powder Technol, (2003) 135–136, 234–242;
[5] H.T. Bi, Electrostatic phenomena in gas–solids fluidized beds, China Particuology, 3(6) (2005) 395–399.
[6] Y. Cheng, D. Y. J. Lau, G. Guan, C. Fushimi, A. Tsutsumi, and C. H. Wang, Experimental and numerical investigations on the electrostatic generations and transport in the downer reactor of a triple bed combined circulating fluidized bed, Industrial and Engineering Chemistry Research, 51(42) (2012) 14258–14267.
[7] F. Fotova, X. T. Bi, and J. R. Grace, Electrostatics in gas-solid fluidized beds, A Review of Chemical Engineering Science, 173 (2017) 303–334.
[8] J. Wu, H. T. Bi, Addition on fines for the reduction of powder charging particles mixers, Advanced Powder Technology, 22(3) (2011) 332–335.
[9] M. Murtomaa, J. Peltonen, and J. Salonen, One step–measurement of powder resistivity as a function of relative humidity and its effect on charging, Journal of Electrostatics, 76(2015) 78–82.
[10] J.N.Chubb, Comment on methods for charges decay measurement, Journal of Electrostatics, 62(1) (2004) 73–80.
[11] J. Sambles, and K. Elsom, The temperature-dependent of electrical resistivity of gold films, Solid State Communications, 52(4) (1984) 367–370.
[12] S.D. Pawar, P. Murugavel, and D. M. Lal, Effect of relative humidity and sea level pressure on the electrical conductivity of air over the Indian Ocean, Journal of Geophysical Research, 114(D2) (2009).
[13] A. Elajnaf, P. Carter, and G. Roley, Electrostatic characterization of inhaled powders; effect of the contact surface and relative humidity, European Journal Pharmaceutical Sciences, 29(2006) 375–384.
[14] G. Rowley., Mackin, L.A., The effect of moisture sorption on electrostatic charging of selected pharmaceutical excipient powders. Powder Technol, (2003) 135–136, 50–58.
[15] J. Guardiola, V. Rojo, and G. Ramos, Influence of particle size fluidization velocity and relative humidity on fluidized bed electrostatic, Journal of Electrostatics, 37 (1996) 1–20.
[16] J. E. Bauerle, Study of solids electrolyte polarization by a complex admittance method, Westinghouse Laboratories Research, Pittsburgh, pa. 15235, USA
[17] N. Guillet, Etude d'un capteur de gaz potentiométrique, influence et role des espèces oxygénées de surface sur la réponse électrique, Ecole Nationale Supérieure de Mines Saint – Etienne, Thèse, (2001).
[18] A. E. Seaver, Surface resistivity of uncoated insulators, Journal of Electrostatics, 63 (2005) 203–222.
[19] R. Sharma, A. S. Biris, R. A. Sims, and M. K. Mazumder, Effect of ambient relative humidity on charge decay properties of polymer powder and on the occurrence of back corona in powder coating, Conference Record of the IEEE Industry Applications Conference, 36th IAS Annual Meeting, 3 (2001) 1961–1965.
[20] L. P. Lefevre, G. Peizier, and Y. Deslandes, Resistivity of green powder compacts, Particulate, Powder Metallurgy, 44(3) (2001) 259–266.
[21] G. Touchard, Technologie des pulvérulents dans les IAA., Collection Sciences et Techniques Agroalimentaires (2003).
[22] J. Yao, and C.–H. Wang, Granular size and shape effect on electrostatics in pneumatic conveying systems, Chemical Engineering Science, 61 (2006) 3858–3874.
[23] A. T. Ndama, P. Guignon, and K. Saleh, Reproducible test to characterize the triboelectric charging of powders during their pneumatic transport, Elsevier, Journal of Electrostatics, 69(3) (2011) 146–156.
[24] R Lalauze., Physico-chimie des interfaces solide-gaz 1 ; concept et méthologie pour l'étude des interactions solide-gaz, Lavoisier Paris,(2006).